

Thermohaline Convection with Two Stable Regimes of Flow

Henry Stommel

To cite this article: Henry Stommel (1961) Thermohaline Convection with Two Stable Regimes of Flow, Tellus, 13:2, 224-230, DOI: [10.3402/tellusa.v13i2.9491](https://doi.org/10.3402/tellusa.v13i2.9491)

To link to this article: <http://dx.doi.org/10.3402/tellusa.v13i2.9491>



© 1961 The Author(s). Published by Taylor and Francis Group LLC



Published online: 15 Dec 2016.



Submit your article to this journal [↗](#)



Article views: 84



View related articles [↗](#)



Citing articles: 28 View citing articles [↗](#)

Thermohaline Convection with Two Stable Regimes of Flow

By HENRY STOMMEL, Pierce Hall, Harvard University, Massachusetts

(Manuscript received January 21, 1961)

Abstract

Free convection between two interconnected reservoirs, due to density differences maintained by heat and salt transfer to the reservoirs, is shown to occur sometimes in two different stable regimes, and may possibly be analogous to certain features of the oceanic circulation.

The density of sea-water is modified while at the surface by two distinct processes: heating and cooling, which change the temperature, and precipitation and evaporation, which change the salinity. In many important oceanic regions these two density modifying processes work contrarily to one another. For example, the water in and above the main thermocline in all subtropical oceans is able to float on top of the denser deep water (we neglect here all consideration of the "salt-fountain" effect) because its density is depressed through surface heating – but the excessive evaporation in these same latitudes is able to increase the salinity of the surface waters to such an extent that in general their density contrast with deep waters is only one half of what it would be on the basis of temperature alone. In some large semiencllosed seas (e.g. Mediterranean and Red Seas) subject to similar surface heating and evaporation, the salinity can have a predominant influence on the density field. By qualitative comparison of these cases we form an impression that the heat transfer mechanism has a more rapid effect on the density of a newly arriving parcel of water, but that in the long run, given sufficient time, evaporation can reverse the thermal influence.

We do not know enough about the details of oceanic circulation to pursue these questions in their full complexity in nature but we can explore their implications in simple idealized systems. That is all we propose to do here.

First, let us consider a very simple system: a vessel of water stirred so as to maintain uniform temperature T and salinity S . (fig. 1). The walls of the vessel are made of a porous

substance which permits transfer of heat and salt in a simple linear fashion:

$$\frac{dT}{dt} = c(T - T')$$

$$\frac{dS}{dt} = d(S - S')$$

T and S are the temperature and salinity outside the wall and are regarded as fixed.

The equations may be made non-dimensional if we introduce

$$\tau = ct, \quad \delta = \frac{d}{c}, \quad \gamma = T/T', \quad x = S/S':$$

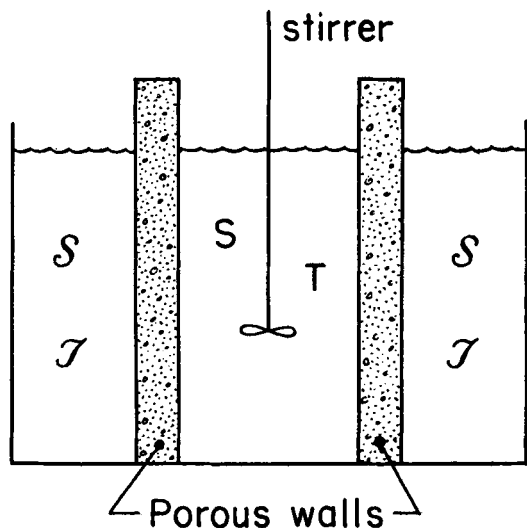


Fig. 1. The idealized experiment, consisting of a well stirred vessel of water with temperature T and salinity S (in general variable in time) separated by porous walls from and outside vessel whose temperature T' and salinity S' are maintained at constant values.

$$\frac{dy}{d\tau} = 1 - y$$

$$\frac{dx}{d\tau} = \delta(1 - x)$$

The quantity δ is considered to be a small quantity, that is we are most interested in situations where the salinity transfer coefficient d is less than the temperature transfer coefficient c , or $\delta < 1$. No matter what the initial values of x and y —say x_0 and y_0 at $\tau = 0$ —the initial final equilibrium state as $\tau \rightarrow \infty$ is $x = 1$, $y = 1$, the solutions of the above equations being, in general

$$y = 1 + (y_0 - 1)e^{-\tau}$$

$$x = 1 + (x_0 - 1)e^{-\delta\tau}$$

Moreover, the temperature approaches its asymptotic value more quickly than the salinity.

Now let us consider a simple form of equation of state

$$\rho = \rho_0(1 - \alpha T + \beta S)$$

which, when expressed in terms of the non-dimensional quantities x and y is

$$\rho = \rho_0 [(1 + (\alpha T) (-y + Rx)]$$

where $R = \beta S / \alpha T$, a measure of the ratio of the effect of salinity and temperature on the density in the final equilibrium state $x = 1$, $y = 1$. We are interested primarily in cases where $R > 1$, because this corresponds to the case where the density at $x = 1$, $y = 1$ is greater than that at $x = 0$, $y = 0$. The time rate of change of density at any time is

$$\frac{d\rho}{dt} = \rho_0 T [-1 + y + R\delta(1 - x)]$$

If in the special case $x_0 = y_0 = 0$, the quantity $R\delta < 1$, but $R > 1$ then in the beginning at $\tau = 0$ the density at first decreases, but eventually increases again until at $\tau = \infty$ it is greater than at the beginning. The entire process can easily be visualized on an S, T diagram or in non-dimensional terms, the x, y plane. In figure 2, the lines of constant density anomaly

$\sigma = \left(\frac{\rho}{\rho_0} - 1\right) / (\alpha T)$ are drawn for the case $R = 2$.

The density anomaly is 0 at the initial condition $x = 0$, $y = 0$, and at the asymptotic limit $\tau \rightarrow \infty$,

Tellus XIII (1961), 2

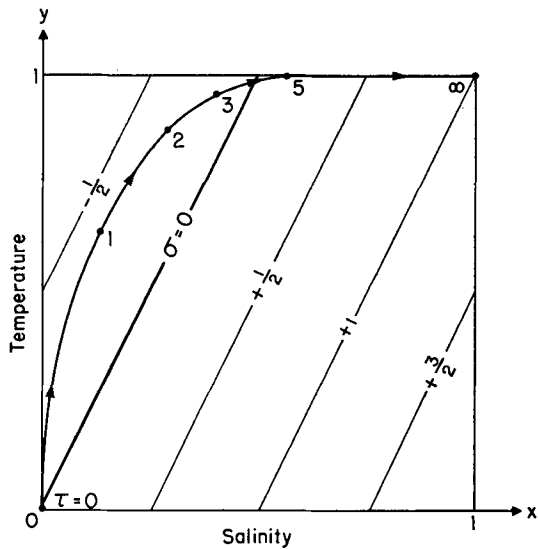


Fig. 2. Non-dimensional salinity-temperature diagram show lines of constant density (σ is density anomaly) for the case $R = 2$. The points marked $\tau = 0, 1, 2, 3, 5, \infty$ illustrate values of temperature and salinity at successive instants of time for $\delta = 1/6$.

the density anomaly is $+1$, therefore the fluid in the time dependent process in the case where $\delta = 1/6$ are plotted as points along a curve for increasing τ . During the early stages the density decreases, until at $\tau = 1$ it begins to increase again. At about $\tau = 4$ the density is back at its initial value and henceforth increases to its asymptotic limit as $\tau \rightarrow \infty$.

Another way of visualizing the different rates of the salt and temperature transfer processes in controlling the density is to consider a simple steady state process, in which water at $T = 0$, $S = 0$ flows into the vessel at rate q , and the mixture is withdrawn at the same rate. The arrangement for this experiment is shown in figure 3. The equations describing this state are

$$\frac{dT}{dt} = 0 = c(T - T_0) - qT$$

$$\frac{dS}{dt} = 0 = d(S - S_0) - qS$$

and reduced to non-dimensional form as before

$$1 - (1 + f)y = 0$$

$$\delta - (\delta + f)x = 0$$

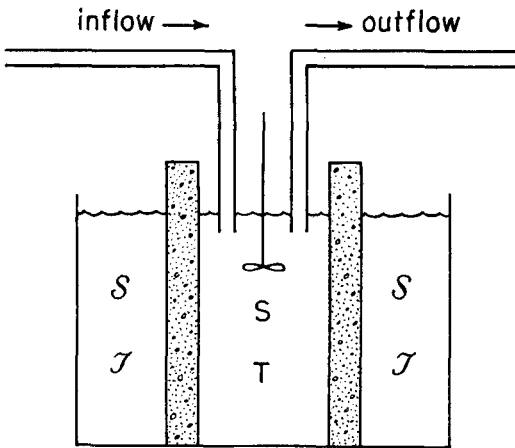


Fig. 3. The idealized steady state experiment.

where $f' = q/c$ denotes a dimensionless flow rate. The equilibrium values of x , y which obtain in the vessel are

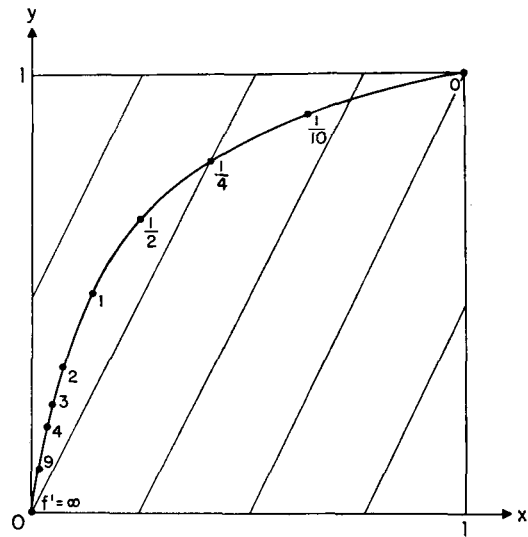
$$y = \frac{1}{1 + f'}$$

$$x = \frac{1}{1 + \frac{f'}{\delta}}$$

The water which enters the vessel has zero density anomaly. When it leaves its density may be greater or less than that entering depending upon the flow rate f' . The points x , y corresponding to the salinity and temperature of the outflow lie along the curve:

$$\frac{1 - y}{y} = \frac{\delta(1 - x)}{x}$$

depicted in figure 4 for the value $\delta = 1/6$. The actual points x , y for certain choices of flow rate f' . The shape of the curve depends only upon δ . The position of the points x , y on this curve depends only on f' . If we now choose $R = 2$ as before we can draw the same lines of density anomaly as in figure 2. Hence the most dense outflow occurs for very small discharge rates $f' \rightarrow 0$, the outflowing water being denser than that flowing into the vessel. On the other hand, the position of points for which $1/4 < f' \leq \infty$ indicates that in this range of discharge the outflow is less dense than the inflow. The purpose of

Fig. 4. Values of non-dimensional temperature y and salinity x for steady state experiment (fig. 3) for different rates of flow, f' .

exploring these extremely simple models has been to lay a groundwork for the remarks made in the introduction where it was stated that the very different density structure in the Atlantic and Mediterranean might be simply due to different rates of flow, but the models are obviously too idealized for direct application to natural conditions.

They are, however, suitable to use as a basis for exploring further consequences of the density transforming processes: in particular the fact that the flow rates in free convective systems depend upon the density differences themselves. There is a kind of "feedback" of the density difference produced upon the flow rate which produces it, that now must be introduced into the system in a simple way. The easiest way to accomplish this is to introduce another stirred vessel surrounded by a reservoir at $-T$, and $-S$, as shown in figure 5.

The two vessels are connected by a large overflow at the top so that free surface of water is level across the top of each vessel. Connecting them at the bottom is a capillary tube whose resistance k is such that the flow q in the tube is directed from the high pressure (high density) vessel toward the low pressure (low density) vessel by a simple linear law

$$kq = \rho_1 - \rho_2$$

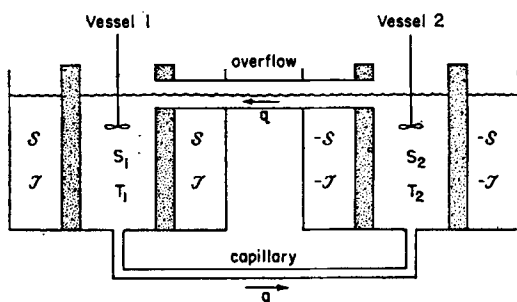


Fig. 5. Two vessel experiment, with rate of flow, q , through capillary determined by the density difference between the two vessels. The upper overflow is provided so that the surface level in each vessel remains the same. The density difference between the two vessels depends on the flow rate as well as the nature of the transfer through the walls.

The flow q is positive if directed from vessel 1 to vessel 2, and negative otherwise. There is, of course, a counterflow of the same amount returning through the overflow, so that the volume of water in each vessel remains the same.

We are concerned with solution of symmetric form, so we can define a single temperature $T = T_1 = -T_2$ and a single salinity $S = S_1 = -S_2$, so that the laws for conservation of temperature and salinity are simply

$$\frac{dT}{dt} = c(T - T) - |2q|T$$

$$\frac{dS}{dt} = d(S - S) - |2q|S$$

It is important to note that in the second term on the right hand side the flux enters with an absolute value sign. This means that the exchange of properties is insensitive to the direction of the circulation. Introducing the previous notation, and defining

$$f = \frac{2q}{c}$$

$$\lambda = \left(\frac{c}{4\rho_0\alpha T} \right) k$$

the appropriate non-dimensional forms of the relations describing the systems are

$$\frac{dy}{d\tau} = 1 - y - |f|y$$

$$\frac{dx}{d\tau} = \delta(1 - x) - |f|x$$

$$\lambda f = (-y + Rx)$$

The last equation implies that the flow in the capillary is in a series of quasi-equilibrium states—since no time derivatives occur in it. Substitution of the last equation into the first two, to eliminate f , yields two non-linear equations

$$\frac{dy}{d\tau} = 1 - y - \frac{y}{\lambda} \left| -y + Rx \right|$$

$$\frac{dx}{d\tau} = \delta(1 - x) - \frac{x}{\lambda} \left| -y + Rx \right|$$

The points of equilibrium correspond to those values of x and y for which $dy/d\tau$ and $dx/d\tau$ vanish, thus leading to a cubic for y in terms of x . There will, therefore, sometimes be three real solutions, or three sets of values of x , y which are equilibrium points. A simple graphical construction enables us to see under what conditions several equilibria are admitted. Solving the first two equations for x and y , in stationary state, we obtain

$$x = \frac{1}{1 + |f|/\delta} \quad y = \frac{1}{1 + |f|}$$

and

$$\lambda f = \phi(f; R, \delta) \equiv \left(-\frac{1}{1 + |f|} + \frac{R}{1 + |f|/\delta} \right)$$

In figure 6 the function $\phi(f; R, \delta)$ has been plotted as a function of f for $R=2$, and for two choices of δ , $\delta=1$, and $\delta=1/6$.

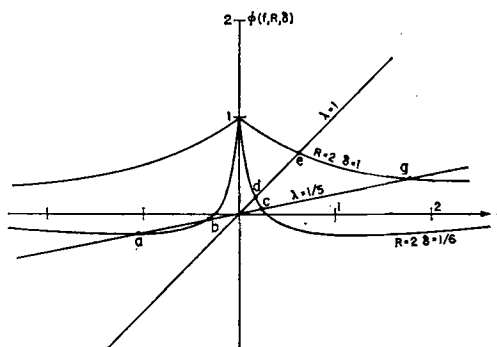


Fig. 6. Graph for determining the equilibria of the two vessel convection experiment (see text).

The solution (or real roots of the cubic) occur where this curve intersects the line λf . Two lines are drawn, one for $\lambda = 1$ and one for $\lambda = 1/5$, λ is defined as positive.

In the case $R=2$, $\delta=1/6$, $\lambda=1/5$ there are three intersections, located at points a , b and c ; the corresponding approximate values of the roots are $f = -1.1$, -0.30 , $+0.23$. These represent three different ways in which the simple convection can occur between the coupled vessels without change in time. With a somewhat larger value of λ the line cuts the function $\phi(f; 2, 1/6)$ in only one point—in the case $\lambda=1$, it cuts at d only.

For certain choices of the parameters R and δ there are forms of $\phi(f; R, \delta)$ for which no choice of λ can produce three real roots. For example, the choice $R=2$, $\delta=1$ gives only one intersection (e or g) for any one choice of λ . It can be seen that this is always true when $\phi(f; R, \delta)$ has no zeros. To explore the limitation on zeros of the ϕ function, we note that if $\phi = 0$ then

$$\frac{1}{1+|f|} = R \frac{1}{1+|f|\delta}$$

or

$$(1-R)\delta = (R\delta-1)|f|$$

Thus the necessary condition for three intersections is

$$R\delta < 1 \quad \text{if } R > 1$$

or

$$R\delta > 1 \quad \text{if } 0 < R < 1$$

To be a sufficient condition λ must also be small enough.

Proceeding now to the x, y plane (dimensionless, S, T diagram) we can draw as before the lines of equal density. These, of course, coincide with the lines of equal flow f in the capillary. In figure 7, the three equilibrium points a , b , c , are located for the particular case $R=2$, $\delta=1/6$, $\lambda=1/5$. The locations are computed from the values of flux f as determined in figure 6. The paths which temperature and salinity follow in the course of approaching equilibrium points can be plotted by the method of isoclines as given in STOKER (1950), a few are sketched in figure 7.

Both a and c are stable equilibrium points. Upon detailed examination by the method of Poincaré it can be shown that point a

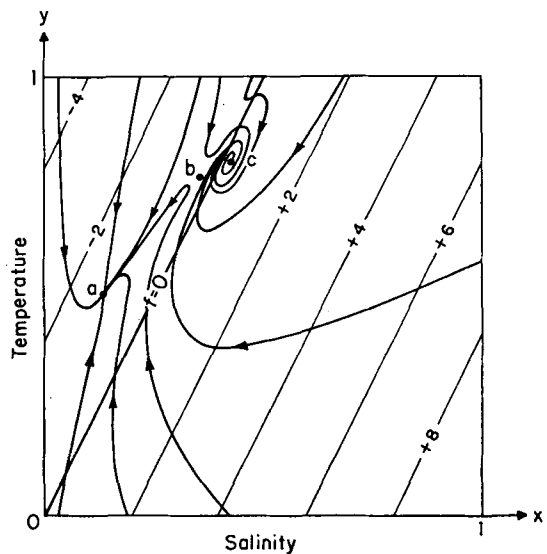


Fig. 7. The three equilibria a , b , and c for the two vessel convection experiment with $R = 2$, $\delta = 1/6$, $\lambda = 1/5$. A few sample integral curves are sketched to show the stable node a , the saddle b , and the stable spiral c .

is a stable node, whereas point c is a stable spiral. Point b on the other hand is a saddle point, so that the system would not stay in that state if perturbed ever so slightly.

A similar sketch for the system where only one equilibrium point (g in figure 6) in the system where $R=2$, $\delta=1$, $\lambda=1/5$ is shown in figure 8. It is a single stable node.

The fact that even in a very simple convective system, such as here described, two distinct stable regimes can occur (as in figure 7)—one (point a) where temperature differences dominate the density differences and the flow through the capillary is from the cold to the warm vessel, and the other where salinity dominates the density difference so that the flow in the capillary is opposite, from warm to cold—suggests that a similar situation may exist somewhere in nature. One wonders whether other quite different states of flow are permissible in the ocean or some estuaries and if such a system might jump into one of these with a sufficient perturbation. If so, the system is inherently fraught with possibilities for speculation about climatic change. Such a perturbation could be in the momentary state of the system—with all parameters remaining constant, or it could

be a slight change in the parameters. Referring to figure 6 to see the effect of a slight increase in λ we see that if λ were to become slightly greater than $1/4$, the two intersections a and b would vanish. Thus, in the system depicted in figure 6, a slight change in λ could cause the temperature dominated circulation at a to jump over to the reverse salinity circulation at c , and it would then stay there even when λ was restored to its original value.

Appendix

The question of the stability of the equilibrium points is difficult to decide by graphical construction. We let $x = \bar{X} + x'$, $y = \bar{Y} + y'$ where \bar{X} and \bar{Y} are values at a particular equilibrium point; hence they satisfy the relation

$$0 = 1 - \bar{Y} - \frac{\bar{Y}}{\lambda} |\bar{Y} - R\bar{X}|$$

$$0 = \delta (1 - \bar{X} - \frac{\bar{X}}{\lambda} |\bar{Y} - R\bar{X}|)$$

The quantities x' and y' are regarded as small departures from \bar{X} and \bar{Y} and we form a linearized expression for $dx'/d\tau$ and $dy'/d\tau$ which is valid in the neighborhood of \bar{X} , \bar{Y} by substitution and dropping all products of x' , y' .

Moreover it is necessary to distinguish between two cases: (1) where the values $\bar{Y} > R\bar{X}$, (2) where $\bar{Y} < R\bar{X}$. Equilibrium points in case (1) have negative f , in case (2) positive f . One must allow, in this way for the absolute value sign. Forming the quotient of the two linearized perturbation equations, leads to the general form

$$\frac{dy'}{dx'} = \frac{ax' + by'}{cx' + dy'}$$

where the coefficients a , b , c , d are defined separately for the two cases as follows

	Case (1) $\bar{Y} > R\bar{X}$ $f < 0$	Case (2) $\bar{Y} < R\bar{X}$ $f > 0$
a	$R\bar{Y}/\lambda$	$-R\bar{Y}/\lambda$
b	$-1 - (2\bar{Y} - R\bar{X})/\lambda$	$-1 + (2\bar{Y} - R\bar{X})/\lambda$
c	$-\delta + (2R\bar{X} - \bar{Y})/\lambda$	$-\delta - (2R\bar{X} - \bar{Y})/\lambda$
d	$-\bar{X}/\lambda$	\bar{X}/λ

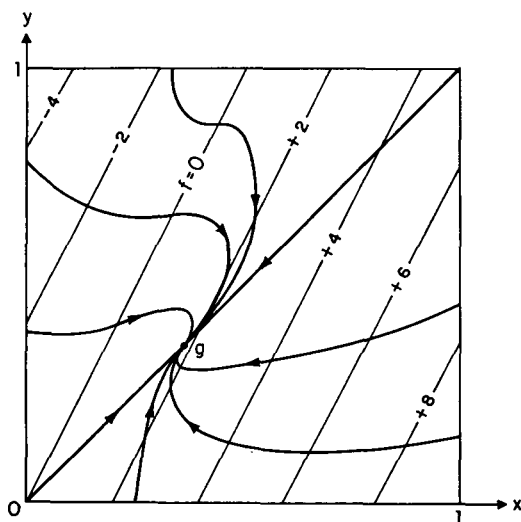


Fig. 8. The single stable node g for the case $R=2$, $\delta=1$, $\lambda=1/5$.

Table I. Numerical Calculations on Stability of Equilibrium Points.

System	$R = 2$	$\delta = 1/6$	$\lambda = 1/5$	$R = 2 \quad \delta = 1 \quad \lambda = 1/5$
f	-1.10	-0.30	+0.23	+1.76
Case	(1)	(1)	(2)	(2)
\bar{X}	0.13	0.36	0.42	0.36
\bar{Y}	0.48	0.77	0.81	0.36
a	4.80	7.70	-8.10	-3.60
b	-4.50	-5.10	2.90	-1.00
c	0.03	3.18	-4.52	-6.40
d	-0.65	-1.80	2.10	1.80
$(b-c)^2$	20.5	68.4	55.0	29.1
$4ad$	-12.5	-55.5	-68.1	-25.9
$(b-c)^2 + 4ad$	8.0	12.9	-13.1	3.2
ad	-3.12	-13.8	—	-6.48
bc	-0.13	-16.2	—	6.40
$ad-bc$	-2.99	2.4	—	-0.08
$b+c$	-4.47	-1.92	-1.62	-7.40
Poincaré Type	I(A) Stable node	I(B) Saddle	II(B) Stable spiral	I(A) Stable node

The Poincaré conditions on the form of the equilibrium points are (STOKER, 1950)

$$\text{Type I } (b-c)^2 + 4ad > 0 \begin{cases} \text{(A) Node if } ad - bc < 0 \\ \text{(B) Saddle if } ad - bc > 0 \end{cases} \begin{cases} \text{Stable if } b+c < 0 \\ \text{Unstable if } b+c > 0 \end{cases}$$

$$\text{Type II } (b-c)^2 + 4ad < 0 \begin{cases} \text{(A) Center if } b+c = 0 \\ \text{(B) Spiral if } b+c \neq 0 \end{cases} \begin{cases} \text{Stable if } b+c < 0 \\ \text{Unstable if } b+c > 0 \end{cases}$$

$$\text{Type III } (b-c)^2 + 4ad = 0 \quad \text{Node} \begin{cases} \text{Stable if } b+c < 0 \\ \text{Unstable if } b+c > 0 \end{cases}$$

The numerical values of all quantities are calculated in Table I for the systems shown in figures 7 and 8.

REFERENCE

STOKER, J. J., 1950: *Nonlinear Vibrations*, Interscience Publisher, New York, 273 pp.